JACS
JOURNAL OF THE AMERICAN CHEMICAL SOCIETY
Communication
pubs.acs.org/JACS

Weak Ferromagnetic Ordering of the $Li^+[TCNE]^{\bullet-}$ (TCNE = Tetracyanoethylene) Organic Magnet with an Interpenetrating Diamondoid Structure

Jae-Hyuk Her,[‡,¶] Peter W. Stephens,*[,‡] Royce A. Davidson,[#] Kil Sik Min,[#,§] Joshua D. Bagnato,[#,&] Kipp van Schooten,[†] Christoph Boehme,[†] and Joel S. Miller*[,#]

[#]Department of Chemistry, University of Utah, 315 South 1400 East, Salt Lake City, Utah 84112-0850, United States
[†]Department of Physics & Astronomy, University of Utah, 115 South 1400 East, Salt Lake City, Utah 84112-0830, United States
[‡]Department of Physics & Astronomy, Stony Brook University, Stony Brook, New York 11794-3800, United States

Supporting Information

ABSTRACT: Li[TCNE] (TCNE = tetracyanoethylene) magnetically orders as a weak ferromagnet (canted antiferromagnet) below 21.0 ± 0.1 K, as observed from the bifurcation of the field-cooled and zero-field-cooled magnetizations, as well as remnant magnetization. The structure, determined *ab initio* from synchrotron X-ray powder diffraction data, consists of a planar μ_4-$[TCNE]^{\bullet-}$ bound to four tetrahedral Li^+ ions. The structure consists of two interpenetrating diamondoid sublattices, with closest interlattice distances of 3.43 and 3.48 Å. At 5 K this magnetic state is characterized by a coercivity of ~30 Oe, a remnant magnetization of 10 emu·Oe/mol, and a canting angle of 0.5°.

Tetracyanoethylene (TCNE) plays an important role in the development of organic-based magnetic materials. Magnetically ordered materials with T_c's up to 127 °C occur in compounds in which the $[TCNE]^{\bullet-}$ radical anion coordinates to paramagnetic transition metal ions. In all cases, the $[TCNE]^{\bullet-}$ $S = {}^1/_2$ spins couple with spins on high-spin transition metal ions.[1−4] These materials can possess 0-, 1-, 2-, and 3-D extended structures with $S = {}^1/_2$ $[TCNE]^{\bullet-}$, μ-$[TCNE]^{\bullet-}$, μ_4-$[TCNE]^{\bullet-}$, and μ_4-$[TCNE]^{\bullet-}$, respectively.

Additionally, for alkali cations,[5−7] $[TCNE]^{\bullet-}$ dimerizes as diamagnetic π-$[TCNE]_2^{2-}$ with exceptionally long (~2.9 Å)[8,9] two-electron, four-center (2e⁻/4c) C−C bonds.[10] As part of our systematic exploration of the unusual bonding associated with the $[TCNE]_2^{2-}$ dimer, we unexpectedly discovered a new structural motif and magnetic ordering as a weak ferromagnet for $Li^+[TCNE]^-$.

The reaction of TCNE and LiI forms a dark green product,[11] with IR ν_{CN} absorptions at 2280, 2221, 2177, and 2137 cm^{-1} that are inconsistent with the presence of either isolated $[TCNE]_2^{2-}$ or $[TCNE]^{\bullet-}$,[12] but virtually identical to those reported for $[Fe^{II}(TCNE)(NCMe)_2][Fe^{III}Cl_4]$ (i.e., 2222 and 2178 cm^{-1}), which possesses μ_4-$[TCNE]^{\bullet-}$.[2] The blue shift of the more intense 2221 and 2177 cm^{-1} ν_{CN} absorptions with respect to 2183 and 2144 cm^{-1} that are present for isolated $[TCNE]^{\bullet-}$ [12] is expected due to the $Li^+\cdots N$ interaction.[13] Backbonding arising from d_π−$\pi^*\{[TCNE]^{\bullet-}\}$ overlap, and leading to a red shift of the ν_{CN} absorptions, cannot occur as Li^+ lacks low-lying d orbitals, and this does not occur for $[Fe(TCNE)(NCMe)_2][FeCl_4]$. The single δ_{CCN} absorption at 525 cm^{-1} is also in accord with $[TCNE]^{\bullet-}$ (521 cm^{-1}), but it is not split into three bands as occurs for $[TCNE]_2^{2-}$.[10] While single crystals sufficient for a structure determination could not be isolated, X-ray powder diffraction (XRPD) was observed.

High-resolution XRPD patterns were collected at beamline X16C of the National Synchrotron Light Source at ambient temperature, 250, 200, 150, 100, 50, 20, and 16 K (Figure S1; Table S1).[14,15] The structure was determined by simulated annealing and Rietveld refinement (Figure 1), and reveals planar μ_4-$[TCNE]^{\bullet-}$ bound to four tetrahedral Li^+ ions (Figure 2a). The structures at all of the temperatures studied are isomorphous, and no evidence was found for a structural phase transition. Each Li^+ is tetrahedrally surrounded by four $[TCNE]^{\bullet-}$'s (Figure 2b) with the central CC and C−CN distances of 1.41(1) and 1.51(1) Å at 16 K, and the average Li−

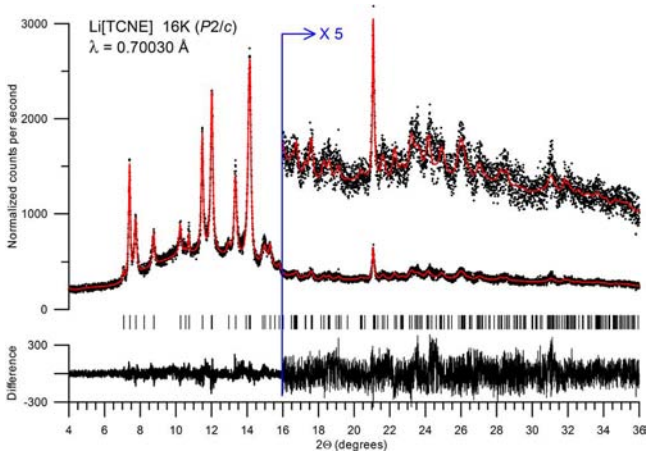

Figure 1. High-resolution synchrotron powder diffraction data (black dots) and Rietveld fit for the refined structure of Li[TCNE] at 16 K (red solid line). The lower trace is the difference, measured minus calculated, plotted to the same vertical scale. The results of similar fits at other temperatures are given in the Supporting Information.

Received: October 22, 2013
Published: November 21, 2013

   dx.doi.org/10.1021/ja410818e | J. Am. Chem. Soc. 2013, 135, 18060−18063

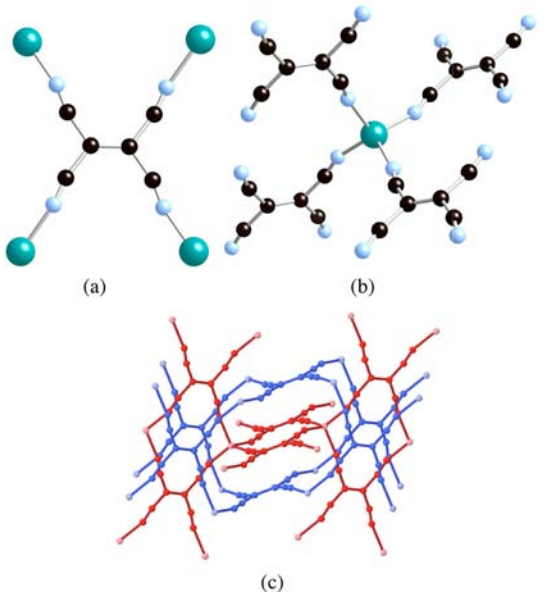

Figure 2. Structure of planar μ_4-$[TCNE]^{\bullet-}$ bound to four Li^+ ions (a), and tetrahedral geometry of four $[TCNE]^{\bullet-}$'s surrounding a Li^+ ion (b). Li is green, C black, and N blue. The extended 3-D network structure of Li[TCNE], with the two interpenetrating diamondoid lattices in red and blue, is shown in (c). Li^+ is shown as a lighter tint than C and N in each sublattice.

N distance of 2.05 Å; N–Li–N angles range from 98° to 121°, and Li^+-bridged N···N distances range from 3.22 to 3.46 Å (Table S2). Albeit noncubic, this arrangement forms an extended 3-D diamondoid topology equivalent to zinc-blende, as well as PbS as observed for $(NMe_4)Cu^{II}[Pt^{II}(CN)_4]$.[16] The large separation between Li^+ ions across $[TCNE]^{\bullet-}$ (6.30 and 7.67 Å) accommodates a second, interpenetrating lattice (Figure 2c). Interpenetrating independent 3-D diamondoid lattices have also been observed for cubic $M(CN)_2$ (M = Mn, Zn, Cd).[17] The shortest inter-sublattice central C···C separations are 5.41 and 5.43 Å along the *b* and *a* axes, respectively. The shortest interlattice C···N and C···C separations are 3.46 and 3.28 Å, respectively.

In accord with the presence of $S = {}^1/_2$ $[TCNE]^{\bullet-}$, the 280 K pulsed electron paramagnetic resonance (EPR) spectra revealed a featureless absorption centered at $g = 2.0038(7)$, with a shift to $g = 2.0041(7)$ at 77 K, but no EPR center observed at 9.5 K. This is consistent with a free electron behavior within the paramagnetic phase in good agreement with solution spectra reported for $[TCNE]^{\bullet-}$ as the sodium salt with $g = 2.0026(2)$.[18,19]

The magnetization, $M(T)$, at 1000 Oe was measured between 5 and 400 K under an inert atmosphere using a Quantum Design MPMS-5XL 5 T SQUID magnetometer equipped with a reciprocating sample measurement system as previously described,[20,21] and χ (= M/H) is displayed as $\chi T(T)$, $\chi^{-1}(T)$, and $\chi(T)$,[22] Figure 3. Above 120 K, $\chi^{-1}(T)$ is linear and can be fit to the Curie–Weiss expression, $\chi = C(T - \theta)^{-1}$ (C and θ are the Curie and Weiss constants, respectively) with $\theta = -39$ K, Figure 3, indicating significant antiferromagnetic coupling. The value of C is 0.375 emu·K/mol, as expected for $S = {}^1/_2$, $g = 2$ material. The magnetization gradually increases with decreasing temperature until it abruptly increases, Figure 3 inset, at 20.2 K [from the $dM(T)/dT$ data].

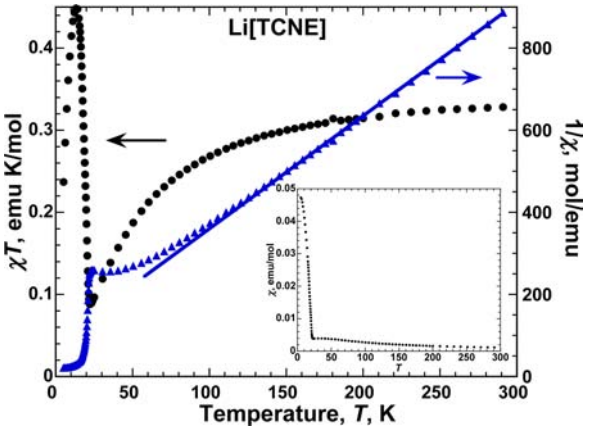

Figure 3. $\chi T(T)$ (●) and $\chi^{-1}(T)$ (▲) for Li[TCNE]. Inset is $\chi = M/H$ (H = 1000 Oe). The line is the fit to $\chi = C(T - \theta)^{-1}$ with $\theta = -39$ K.

Below 120 K, $\chi(T)$ is less than that expected for Curie–Weiss behavior with $\theta = -39$ K. This is indicative of significant spin coupling between the $[TCNE]^{\bullet-}$ sites. Unexpectedly, below 22 K, $\chi T(T)$ abruptly increases with decreasing temperature, reaching a maximum of 0.45 emu·K/mol at 13.1 K, before decreasing again upon further cooling, Figure 3. Likewise, $\chi(T)$ has an abrupt increase, Figure 3 inset, and $\chi^{-1}(T)$ has an abrupt decrease at 22.3 K. These data suggest magnetic ordering and/or a structural phase transition with a concomitant increase in spin coupling. A Spin-Peirels transition[23] can be ruled out, as this would lead to a diamagnetic ground state, not an increase in susceptibility. The unit cell parameters above and below the 22 K transition temperature (Figure S1; Table S1) are essentially unchanged, arguing against a structural transition, although the quality of data obtainable from these samples admits the possibility of a subtle change.[15]

The 5-Oe field-cooled, $M_{FC}(T)$, and zero-field-cooled, $M_{ZFC}(T)$, magnetizations for Li[TCNE] exhibit a bifurcation, T_b, at 21.1 K (Figure 4), indicative of magnetic ordering. The $M_{FC}(T)$ is nearly coincident with the remnant magnetization, $M_r(T)$, Figure 4. The T_c extrapolated from the temperature at which $M(T,H = 0) = 0$ is 21.0 and 20.9 K from the $M_{FC}(T)$ and $M_r(T)$, respectively, and is in good agreement with T_b.

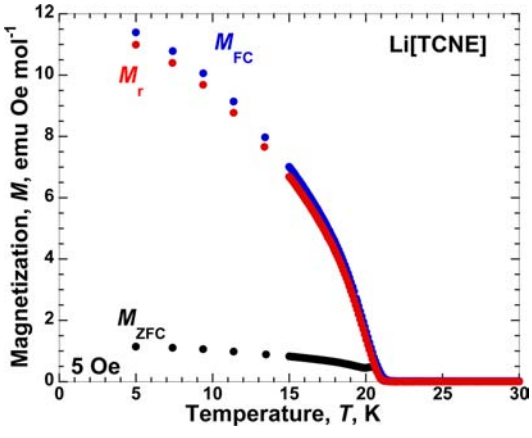

Figure 4. Zero-field-cooled, $M_{ZFC}(T)$, field-cooled, $M_{FC}(T)$, and remnant, $M_r(T)$, magnetizations for Li[TCNE].

dx.doi.org/10.1021/ja410818e | J. Am. Chem. Soc. 2013, 135, 18060–18063

The 5 K $M(H)$ shows a rapid rise with increasing field, H, Figure 5, followed by a linear increase. At 50 kOe the magnetization is 175 emu·Oe/mol and still rising. Hence, it indicates weak ferromagnetic (canted antiferromagnetic behavior). The canting angle, γ, for a polycrystalline sample can be estimated from $\sin(\gamma/2) = 2M_r(T\rightarrow0)/M_s$,[24] with $M_r(T\rightarrow0)$ being obtained by extrapolating the low-temperature remnant magnetization, $M_r(T)$, to 0 K, and is 12 emu·Oe/mol, while M_s is assumed to be 5585 emu·Oe/mol; thus, $\gamma = 0.5°$, in accord with other weak ferromagnetic materials. Li[TCNE] has a coercive field of 30 Oe and remnant magnetization, M_r, of 10 emu·Oe/mol at 5 K, Figure 5.

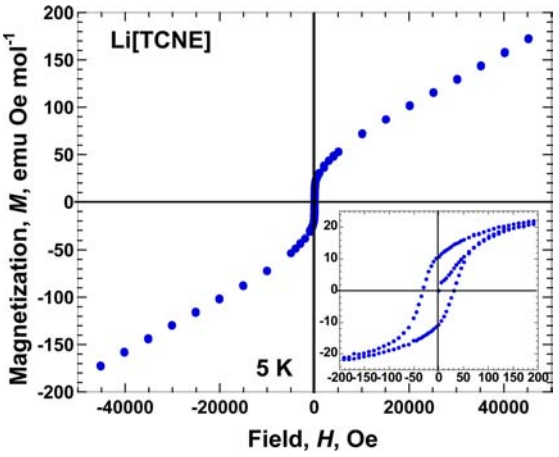

Figure 5. Hysteretic $M(H)$ for Li[TCNE] at 5 K. H_{cr} = 30 Oe, M_r = 10 emu·Oe/mol.

The structure and magnetic data for Li[TCNE] suggest a two-sublattice antiferromagnet, with spins on the two magnetic sublattices slightly canted. At present, it is not known if the distinct diamondoid (structural) networks are the magnetic sublattices (dominant antiferromagnetic coupling along the interlattice C···N interactions), or if there are sites of opposite spin on each sublattice (dominant antiferromagnetic coupling via the N−Li−N bridges). As Li^+ contains only s electrons, superexchange via that route is unexpected. However, superexchange may arise from the covalency of the strong Lewis acid interaction between the Li^+ and N's.

The weak ferromagnetism could arise either from a different anisotropy direction on the two magnetic sublattices or from a Dzyaloshinsky−Moriya interaction.[25] Further work, including pressure studies and AC susceptibility, as well as modeling of the magnetic interactions based on density functional computations is in progress, and should provide insight into these questions.

In conclusion, Li[TCNE] is anomalous with respect to the other alkali salts of $[TCNE]^{\bullet-}$, as it possesses μ_4-$[TCNE]^{\bullet-}$ bound to four tetrahedral Li^+ ions, forming an interpenetrating diamondoid lattice, and not π-$[TCNE]_2^{2-}$. Furthermore, Li^+ does not stabilize μ_4-$[C_4(CN)_8]^{2-}$. Li[TCNE] undergoes a transition from a paramagnetic state to the weak ferromagnetic (canted antiferromagnet) ground state with $T_c = 21.0 \pm 0.1$ K, with a 0.5° canting angle, ∼30 Oe coercivity, and 10 emu·Oe/mol remnant magnetization at 5 K.

Thus, Li[TCNE], consisting only of three first-row elements, has a T_c exceeding those of all reported organic ferromagnets and weak ferromagnets, except 4′-cyanotetrafluorophenyldithiadiazolyl (T_c = 35.5 K).[26] The coercivity is higher than that typically observed for an organic magnet based on first-row elements, and larger than those of all other organic magnets, except those containing Se.[27] This may arise from the noncubic nature of the interpenetrating diamondoid lattices, and is under further investigation.

■ ASSOCIATED CONTENT

Ⓢ Supporting Information

X-ray crystallographic CIF files for Li[TCNE] at eight temperatures between 16 and 295 K, as well as unit cell parameters and selected bond lengths and angles at those temperatures. This material is available free of charge via the Internet at http://pubs.acs.org.

■ AUTHOR INFORMATION

Corresponding Authors

peter.stephens@stonybrook.edu
jsmiller@chem.utah.edu

Present Addresses

[¶]J.-H.H.: GE Global Research Center, 1 Research Circle, Niskayuna, NY 12309
[§]K.S.M.: Kyungpook National University, Daegu, Korea
[&]J.D.B.: Idaho Technology, Inc., Salt Lake City, UT 84106

Notes

The authors declare no competing financial interest.

■ ACKNOWLEDGMENTS

We thank William W. Shum and Endrit Shurdha for their preliminary studies of Li[TCNE], and Rodolphe Clérac (CRPP Bordeaux) and Juan Novoa (Universidad de Barcelona) for helpful discussions. R.A.D., J.D.B., K.S.M., and J.S.M appreciate the continued support by the U.S. Department of Energy Division of Material Science (No. DE-FG03-93ER45504) for chemical synthesis, spectroscopic, and magnetic studies. K.v.S. and C.B. acknowledge support by the NSF MRSEC Grant No. DMR-1121252 CFDA NO. 47.049 for the EPR studies. J.-H.H. and P.W.S. appreciate the National Synchrotron Light Source, Brookhaven National Laboratory, that was supported by the U.S. Department of Energy, Office of Basic Energy Sciences under Contract No. DE-AC02-98CH10886 for the XRPD studies.

■ REFERENCES

(1) (a) Ovcharenko, V. I.; Sagdeev, R. Z. *Russ. Chem. Rev.* **1999**, *68*, 345−363. (b) Blundell, S. J.; Pratt, F. L. *J. Phys.: Condens. Matter* **2004**, *16*, R771−R828. (c) Miller, J. S. *Chem. Soc. Rev.* **2011**, *40*, 3266−2396. (d) Miller, J. S.; Epstein, A. J. *Angew. Chem., Int. Ed.* **1994**, *33*, 385−415. (e) Miller, J. S. *Chem. Soc. Rev.* **2011**, *40*, 3266−3296.
(2) Pokhodnya, K. I.; Bonner, M.; Her, J.-H.; Stephens, P. W.; Miller, J. S. *J. Am. Chem. Soc.* **2006**, *126*, 15592−15593.
(3) Her, J.-H.; Stephens, P. W.; Pokhodnya, K. I.; Bonner, M.; Miller, J. S. *Angew. Chem., Int. Ed.* **2007**, *46*, 1521−1524.
(4) Stone, K. H.; Stephens, P. W.; McConnell, A. C.; Shurdha, E.; Pokhodnya, K. I.; Miller, J. S. *Adv. Mater.* **2010**, *22*, 2514−2519.
(5) Johnson, M. T.; Campana, C. F.; Foxman, B. M.; Desmarais, W.; Vela, M. J.; Miller, J. S. *Chem.—Eur. J.* **2000**, *6*, 1805−1810.
(6) Casado, J.; González, S. R.; Ramírez, F. J.; Navarrete, J. T. L.; Lapidus, S. H.; Stephens, P. W.; Vo, H.-L.; Miller, J. S.; Mota, F.; Novoa, J. J. *Angew. Chem., Int. Ed.* **2013**, *52*, 6421−6425.
(7) Bock, H.; Ruppert, K. *Inorg. Chem.* **1992**, *31*, 5094−5099.
(8) Kaupp, G.; Boy, J. *Angew. Chem., Int. Ed.* **1997**, *36*, 48−49.
(9) Toda, F. *Eur. J. Org. Chem.* **2000**, 1377−1386.
(10) Miller, J. S.; Novoa, J. J. *Acc. Chem. Res.* **2007**, *40*, 189−196.

(11) To a suspension of TCNE (537 mg, 4.19 mmol) in 20 mL of diethyl ether was added LiI (483 mg, 3.61 mmol) dissolved in 1 mL of MeCN slowly, and the mixture was stirred for 2 h at room temperature. The dark green precipitate that formed was collected and dried under vacuum (yield: 360 mg; 64%). Numerous attempt of grow crystals from several solvents were unsuccessful. Analysis (calc) for Li[TCNE]: %C = 53.59 (53.37), %N = 41.55 (41.49). IR (KBr): ν_{CN} 2280(w), 2221(m), 2177(m), 2137(w), and 525(m) cm^{-1}. Absorption spectrum (MeCN), λ_{max}, nm (ε_M, L mol^{-1} cm^{-1}): 426 (5300). Absorption spectrum (Nujol), λ_{max}, nm: 202 (sh), 242.

(12) Miller, J. S. *Angew. Chem., Int. Ed.* **2006**, *45*, 2508−2525.

(13) Nakamoto, K. *Infrared and Raman Spectra of Inorganic and Coordination Compounds*, Part B, 5th ed.; Wiley: New York, 1997, pp 105−106.

(14) A Si(111) double-crystal monochromator selected a highly collimated incident beam of 0.70030 Å on the X16C beamline at Brookhaven National Laboratory. The diffracted X-rays were analyzed by a Ge(111) crystal and detected using NaI scintillation counter. The cryostat and capillary were oscillated by 5° during data collection for better averaging of the powder pattern data. TOPAS-Academic was used to solve the Li[TCNE] structure by simulated annealing method. After finding a decent starting model, subsequent Rietveld refinement was also done by TOPAS-Academic with "rigid body" constraint for highly symmetric TCNE molecule. Quoted standard uncertainties were obtained using a bootstrap procedure described in the TOPAS documentation; realistic uncertainties are several times larger than those based purely on counting statistics. *TOPAS V3*: General profile and structure analysis software for powder diffraction data—User's Manual; Bruker AXS: Karlsruhe, Germany; TOPAS-Academic is described and available at http://www.topas-academic.net. Anisotropic peak broadening model: Stephens, P. W. *J. Appl. Crystallogr.* **1999**, *32*, 281−289.

(15) Chemical formula = C_6LiN_4, MW = 135.04 g/mol, space group = *P*2/*c* (No. 13); a = 5.4328(5) Å, b = 5.4112(6) Å, c = 11.914(2) Å, β = 107.70(1)°, V = 333.71(4) $Å^3$, T = 16 K, Z = 2, ρ_{calc} = 1.344 g/cm^3, R_p = 0.053, R_{wp} = 0.063, χ^2 = 2.10. CCDC 965810−965818. See Table S1 for unit cell parameters, and Table S2 for bonding geometry at 16, 50, 100, 150, 200, 250, and 300 K.

(16) Gable, R. W.; Hoskins, B. F.; Robson, R. *J. Chem. Soc., Chem. Commun.* **1990**, 762−763.

(17) Kareis, C. M.; Lapidus, S. H.; Stephens, P. W.; Miller, J. S. *Inorg. Chem.* **2012**, *51*, 3046−3050. Hoskins, B. F.; Robson, R. *J. Am. Chem. Soc.* **1990**, *112*, 1546−1554. Williams, D. J.; Partin, D. E.; Lincoln, F. J.; Kouvetakis, J.; O'Keefe, M. *J. Solid State Chem.* **1997**, *134*, 164−169. Reckeweg, O.; Simon, A. *Z. Naturforsch.* **2002**, *57b*, 895−900.

(18) Phillips, W. D.; Rowell, J. C.; Weissman, S. I. *J. Chem. Phys.* **1960**, *33*, 626−627.

(19) Free induction decay pulsed EPR measurements using a Bruker X-band Elexsys E580 spectrometer were necessitated by the very high density of paramagnetic centers, which otherwise detune the microwave cavity, defeating continuous-wave (cw) operation. The origin of the absence of any detectable EPR or ferromagnetic resonance (FMR) below T_c between 675 and 6175 Oe is unknown. It could be caused by very high spin-relaxation rates or disorder-induced extreme FMR line broadening, which could reduce the strength of the FMR signal below the detection limit.

(20) Brandon, E. J.; Rittenberg, D. K.; Arif, A. M.; Miller, J. S. *Inorg. Chem.* **1998**, *37*, 3376−3384.

(21) Arthur, J. L.; Moore, C. E.; Rheingold, A. L.; Lapidus, S. H.; Stephens, P. W.; Miller, J. S. *Adv. Funct. Mater.* **2012**, *22*, 1802−1811.

(22) The diamagnetic correction used for Li[TCNE] is -64.2×10^{-6} emu/mol. In the paramagnetic phase, 1000 Oe is a small field, and M/H is a good approximation to dM/dH. While not strictly correct, it is customary to refer to M/H as χ even for magnetically ordered phases.

(23) Bray, J. W.; Interrante, L. V.; Jacobs. I. S.; Bonner, J. C. In *Extended Linear Chain Compounds*; Miller, J. S., Ed.; Plenum Pub. Corp.: New York, 1983; Vol. 3, pp 353−415.

(24) Bhowmick, I.; Hillard, E. A.; Dechambenoit, P.; Coulon, C.; Harris, T. D.; Clérac, R. *Chem. Commun.* **2012**, *48*, 9717−9719.

(25) Carlin, R. L. *Magnetochemistry*; Springer-Verlag: Berlin, 1986; pp 150−150.

(26) Banister, A. J.; Bricklebank, N.; Lavender, I.; Rawson, J. M.; Gregory, C. I.; Tanner, B. K.; Clegg, W.; Elsewood, M. R. J.; Palacio, F. *Angew. Chem., Int. Ed.* **1996**, *35*, 2533−2535.

(27) Robertson, C. M.; Leitch, A. A.; Cvrkalj, K.; Reed, R. W.; Myles, D. J. T.; Dube, P. A.; Oakley, R. T. *J. Am. Chem. Soc.* **2008**, *130*, 8414−8425.